Since January 2020 Elsevier has created a COVID-19 resource centre with free information in English and Mandarin on the novel coronavirus COVID-19. The COVID-19 resource centre is hosted on Elsevier Connect, the company's public news and information website.

Virus Research 287 (2020) 198105

Contents lists available at ScienceDirect

Virus Research

journal homepage: www.elsevier.com/locate/virusres

Host antiviral protein IFITM2 restricts pseudorabies virus replication

Jingying Xie[a,b], Yingjie Bi[b], Shujuan Xu[b], Yumei Han[b], Adi Idris[c], Haixia Zhang[b], Xiangrong Li[b], Jialin Bai[b], Yong Zhang[a,**], Ruofei Feng[b,*]

[a] College of Veterinary Medicine, Gansu Agricultural University, No.1 Yingmencun, Lanzhou, 730070, China
[b] Key Laboratory of Biotechnology and Bioengineering of State Ethnic Affairs Commission, Biomedical Research Center, Northwest Minzu University, Lanzhou 730030, China
[c] Menzies Health Institute Queensland, School of Medical Science, Griffith University, Southport, Queensland, Australia

ARTICLE INFO

Keywords:
Pseudorabies virus
IFITM proteins
Cholesterol

ABSTRACT

Pseudorabies virus (PRV) is one of the most destructive swine pathogens and leads to huge economic losses to the global pig industry. Type I interferons (IFNs) plays a pivotal role in the innate immune response to virus infection via induction of a series of interferon-stimulated genes (ISGs) expression. IFN-induced transmembrane (IFITM) proteins, a group of ISGs, are important host self-restriction factors, possessing a broad spectrum of antiviral effects. They are known confer resistance to a variety of RNA and DNA viruses. However, little is known about the role of IFITMs in PRV infection. In this study, we show that IFITM is crucial for controlling PRV infection and that IFITM proteins can interfere with PRV cell binding and entry. Furthermore, we showed that IFITM2-mediated inhibition of PRV entry requires the cholesterol pathway. Collectively, these results provide insight into the anti-PRV role of IFITM proteins and this inhibition possible associated with the change of cholesterol in the endosome, further underlying the importance of cholesterol in virus infection.

1. Introduction

The host innate immune response is the first line of defense against viral infections until specific protection can be established by the adaptive immune system. Type I interferons (IFNs) plays a major role in cell immunity by inducing downstream IFN-stimulated genes (ISGs) that encode several antiviral innate immune effectors. Among these ISGs, the IFN-induced transmembrane proteins (IFITMs) are known to inhibit entry of a wide variety of enveloped RNA viruses (Perreira et al., 2013). The family of IFITM proteins (IFITM 1, 2 and 3) are homologous, localized in the plasma and endo-lysosomal membranes, and confer cellular resistance to many viruses (Bailey et al., 2014; Liao et al., 2019; Zhao et al., 2018). The *IFITM* family were first discovered as ISGs in human neuroblastoma cells and their promoters contain one or more IFN stimulated response elements (ISRE), making them sensitive to type I and type II IFNs (Bedford et al., 2019; Friedman et al., 1984; Lewin et al., 1991; Reid et al., 1989). This group of proteins are known to inhibit the replication of a range of RNA viruses that enter the host cell via endocytosis, including the influenza A virus (IAV), West Nile virus (WNV), Dengue virus (DENV) (Brass et al., 2009; Jiang et al., 2010), severe acute respiratory syndrome coronavirus (SARS CoV), hepatitis C virus (HCV), Marburg virus, Ebolavirus and Zika virus (Huang et al., 2011; Liao et al., 2019; Savidis et al., 2016; Wilkins et al., 2013).

Little is known of the effect of IFITMs on DNA viruses. IFITM1 is known to inhibit *Rana grylio* virus (RGV) at the entry stage (Zhu et al., 2013). On the other hand, IFITM1, 2 and 3 has no effect on the replication of other DNA viruses, such as human papillomavirus (HPV), human cytomegalovirus (HCMV) and adenovirus 5 (Ad5) (Warren et al., 2014). Interestingly, expression of IFITM1, 2 and 3 reduces African Swine Fever virus (ASFV) infectivity in Vero cells, with IFITM2 and 3 impacting viral entry (Muñoz-Moreno et al., 2016). The antiviral effect of IFITMs is mainly exerted through the endocytic pathway and affects viral entry in late endosomal compartments (Diamond and Farzan, 2013). To further expand our understanding of the antiviral activity of IFITMs against DNA viruses, we investigated the role of these proteins in the replication cycle of Pseudorabies virus (PRV).

PRV, or suid herpesvirus 1, is a member of the genus *Varicellovirus*, family *Herpesviridae*. PRV is the causative agent of Aujeszky's disease, which results in neurological and respiratory system disorders in young piglets and death of fetuses and/or abortion in pregnant sows (Liu et al., 2018; Yang et al., 2017). PRV is also an excellent model to study general aspects of alphaherpesvirus biology (Pomeranz et al., 2005). PRV

* Corresponding author at: Key Bioengineering and Technology Laboratory of SEAC, Biomedical Research Center, Northwest Minzu University, No.1 Xibeixincun, Lanzhou, 730030, China.
** Corresponding author at: College of Veterinary Medicine, Gansu Agricultural University, No.1 Yingmencun, Lanzhou, 730070, China.
E-mail addresses: zhychy@163.com (Y. Zhang), fengruofei@xbmu.edu.cn (R. Feng).

https://doi.org/10.1016/j.virusres.2020.198105
Received 19 March 2020; Received in revised form 21 July 2020; Accepted 25 July 2020
Available online 31 July 2020

has a double-stranded DNA genome of approximately 150-kb in length and can infect a broad range of wild and domestic animal species, including cattle, sheep, goats, dogs, cats, and many feral species. PRV is a disease of swine, which serve as a reservoir for the virus (Marcaccini et al., 2008; Müller et al., 2011) and the principal source of natural infection for a diverse range of secondary hosts.

Vaccines are widely used to reduce the economic losses caused by PRV infection (Vannier, 1985; Yu et al., 2014). Bartha is an attenuated PRV vaccine strain, derived from a field strain that was isolated in Hungary and attenuated via multiple passages in cultured chicken cells and embryos (Christensen et al., 1992). The Bartha vaccine genome displays several mutations as compared with the genome of wild-type PRV strains, including a large deletion in the unique short (US) region, encompassing the glycoprotein E (*gE*), *gI*, *US9* and *US2* genes (Lamote et al., 2017; Szpara et al., 2011). Although the Bartha vaccine has been highly successful and is well-characterized with respect to its ability to reduce neuropathogenesis, relatively little is known regarding its effect on the immune system.

Evidence suggests that localization of IFITMs and their influence on vesicular compartments are closely linked to their antiviral activities (Mudhasani et al., 2013; Perreira et al., 2013; Wang et al., 2014). Swine IFITM1 is mainly located on the cell surface, whereas IFITM2 and IFITM3 are mainly located in the cytosol (Lanz et al., 2015; Li et al., 2019). Nevertheless, little is known about IFITM-mediated antiviral activity against PRV. Considering that PRV entry and replication relies on low pH-mediated endocytosis (Miller et al., 2019), it would be interesting to investigate whether IFITMs influence vesicular compartments during PRV infection.

Thus, our goal is to determine the effect of IFITMs on PRV replication and to evaluate whether the IFITM proteins affect the early entry steps of PRV infection in PK15 cells using the vaccine strain Bartha-61.

2. Materials and methods

2.1. Cells, viruses and chemicals

The porcine kidney (PK15) and baby hamster kidney (BHK-21) cell lines were maintained in Dulbecco's modified Eagle's medium (DMEM) supplemented with10 % newborn bovine serum (NBS) at 37 °C/5 % CO_2. IFN-α2a (Sunshine Pharmaceuticals CO., Ltd, Shenyang, China) was used for IFN stimulation. Methyl-β-cyclodextrin (MβCDX; Sigma) used as cholesterol consumers. PF429242 dihydrochloride (Sigma) served as cholesterol pathway inhibitor. PRV Bartha is an attenuated vaccine strain, obtained by extensive passaging of an Aujeszky strain isolated in Hungary (Christensen LS, et al., 1992). Bartha-61 was propagated in BHK-21 cells, and the supernatants of infected cells were clarified and stored at −80 °C.

2.2. Antibodies

Mouse monoclonal antibodies specific for Myc, β-actin and GAPDH were purchased from Abcam. Rabbit polyclonal antibodies specific for IFITM2 and IFITM3 were purchased from Proteintech. Rabbit anti-IFITM1 polyclonal antibody was purchased from Bioss.

2.3. Viral infection and inhibitor studies

The PK15 cell lines were left untreated or treated with IFN-α2a (5000 IU/mL) for 8 h. The cells were then infected with PRV at 100$TCID_{50}$. After 2 h, the viral inoculum was removed, and the infected cells were washed twice with 1 × PBS (pH 7.4) and DMEM containing 3 % NBS was replaced. At various time points post-infection, cell-free culture supernatants and lysates were harvested and stored at −80 °C until use. For PF429242 studies, cells were pretreated for 24 h before infection as previously described (Petersen et al., 2014). All infections were carried out in the continued presence of drug or DMSO, for the length of the infection. For MβCDX studies, cells were pretreated for 45 min and washed prior to infection. Cells were infected with PRV at 100$TCID_{50}$ by adding 1 mL of inoculum to a 6 well dish for two hours at 37 °C. Viral inoculum was removed, cells were overlaid with fresh media except MβCDX. Cells and supernatant were harvested at indicated times for RT-qPCR and virus titer detection.

Table 1
Primers for PCR and RT-qPCR.

Primer Sequence (5′-3′)
IFITM1-F1 CG GGA TCC ATG ATC AAG AGC CAG CAC GA
IFITM1-R1 CG GAA TTC GTA GCC TCT GTT ACT CTT TGC
IFITM2-F2 CG GGA TCC ATG AAC TGC GCT TCC CAG CC
IFITM2-R2 CG GAA TTC GTA GCC TCT GTT ACT CTT TGC
IFITM3-F3 CG GGA TCC ATG AAC TGC GCT TCC CAG CCC
IFITM3-R3 CG GAA TTC GTA GCC TCT GTA ATC CTT TAT
IFITM1-qF TGGCTTTCGCCTACTCCG
IFITM1-qR ACAGTGGCTCCGATGGTCAG
IFITM2-qF TGCCTCCACCGCCAAGT
IFITM2-qR GTGGCTCCGATGGTCAGAAT
IFITM3-qF GAAGATGGTGGGAGACATCATT
IFITM3-qR GAAAATTACCAGGGAGCCAGT
β-actin-qF CAAGGACCTCTACGCCAACAC
β-actin-qR TGGAGGCGCGATGATCTT
PRV-qF GTCAGGAGGCAGTTGTAGGC
PRV-qR CGGACCTCGTGAACTACCC
PRV-probe 5′-(FAM)CCACGGCCGTCACGA-(Eclipse)-3′

2.4. Western blotting

The IFITM genes were amplified from PK15 cells, pretreated with IFN-α2a for 8 h, using specific primers (Table 1). The PCR products were digested and ligated into the pCMV-Myc vector to generate the expression plasmids, Myc-IFITM1, Myc-IFITM2 and Myc-IFITM3. Subsequently, PK15 cells were transfected with the expression plasmids using Lipofectamine® 3000 reagent according to the manufacturer's instructions. Cells were harvested and whole-cell extracts were prepared from cells lysed with lysis buffer containing 50 mM Tris/HCl, pH 7.4, 150 mM NaCl, 1 mM EDTA, 0.25 % sodium deoxycholate, 1 % Triton X-100 and the PMSF protease inhibitor (Beyotime, Shanghai, China). Cell extracts were subjected to 15 % SDS-PAGE, and the separated proteins were transferred to PVDF membranes (Millipore). The non-specific antibody binding sites were blocked with skimmed milk diluted in PBS/Tween® 20 and then incubated with the specific primary and HRP (horseradish peroxidase)-conjugated secondary antibodies. GAPDH or β-actin was used as a loading control. The proteins were detected using ECL reagent (DAKEWE, Beijing, China).

2.5. RNA extraction and RT-qPCR

Cellular RNA was isolated using TRIzol® reagent (Life Technologies). Total RNA (1 μg) was reverse-transcribed to cDNA. Two-step RT-qPCR was performed in a SYBR® Green assay using an Applied Biosystems Master Mix kit in an ABI 7500 Real-Time PCR system. β-Actin was used as the internal control. All experiments were performed using the following amplification profile: one cycle at 94 °C for 30 s and 40 cycles at 94 °C for 5 s and 60 °C for 34 s. Primers used in RT-qPCR were list in Table 1.

2.6. Detection of PRV genome by quantitative PCR

Quantitation of the number of PRV genome copies was achieved by RT-qPCR using specific primers and a Premix ExTaq (TM) (Takara). Fluorescent probes were used to amplify a region of the UL37 PRV gene. Viral DNA from mock-infected or infected with 100$TCID_{50}$ PRV was isolated at 24 h using Viral Genomic DNA Extraction Kit (TIANGEN)

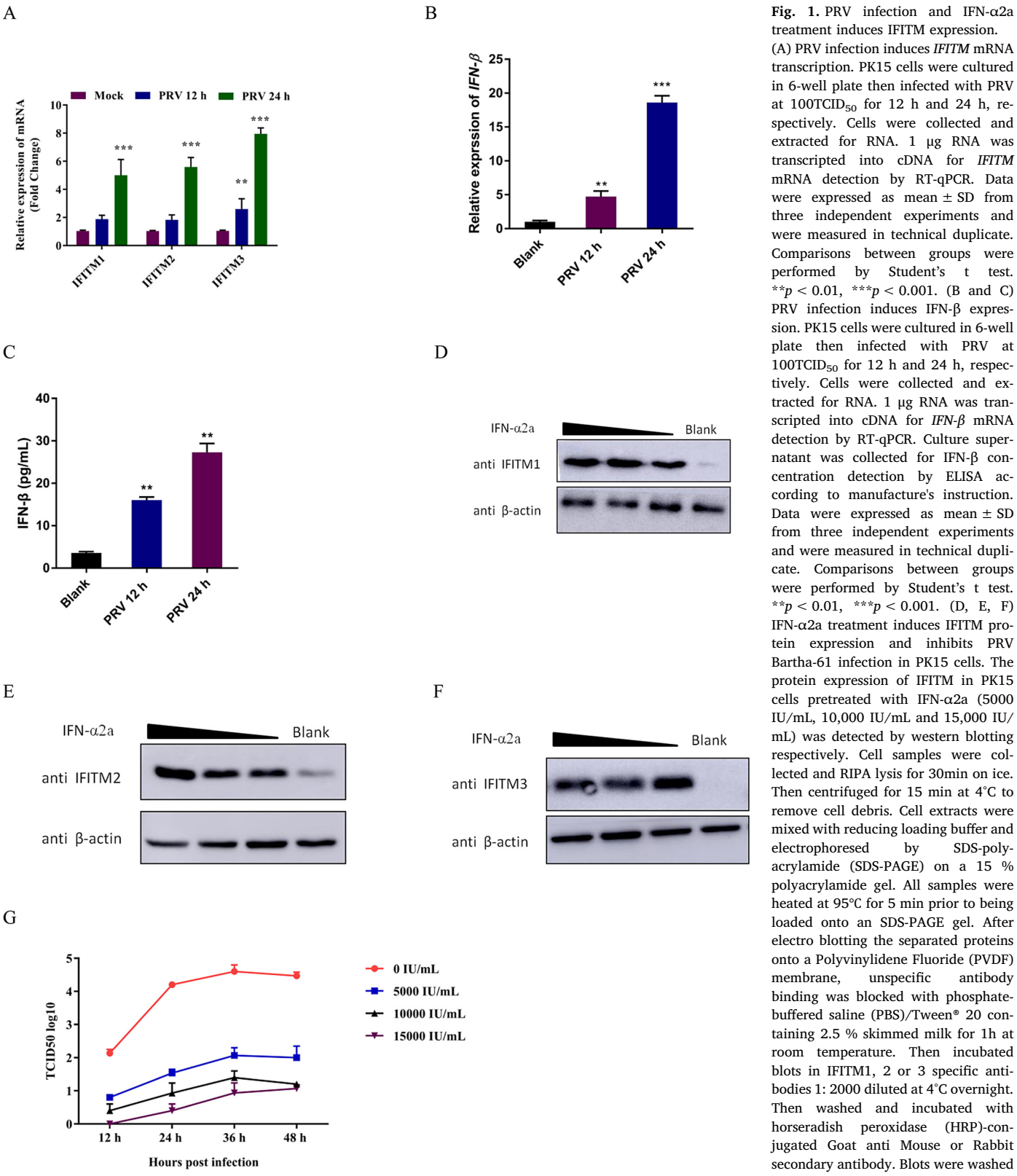

Fig. 1. PRV infection and IFN-α2a treatment induces IFITM expression. (A) PRV infection induces *IFITM* mRNA transcription. PK15 cells were cultured in 6-well plate then infected with PRV at 100TCID$_{50}$ for 12 h and 24 h, respectively. Cells were collected and extracted for RNA. 1 μg RNA was transcripted into cDNA for *IFITM* mRNA detection by RT-qPCR. Data were expressed as mean ± SD from three independent experiments and were measured in technical duplicate. Comparisons between groups were performed by Student's t test. $^{**}p < 0.01$, $^{***}p < 0.001$. (B and C) PRV infection induces IFN-β expression. PK15 cells were cultured in 6-well plate then infected with PRV at 100TCID$_{50}$ for 12 h and 24 h, respectively. Cells were collected and extracted for RNA. 1 μg RNA was transcripted into cDNA for *IFN-β* mRNA detection by RT-qPCR. Culture supernatant was collected for IFN-β concentration detection by ELISA according to manufacture's instruction. Data were expressed as mean ± SD from three independent experiments and were measured in technical duplicate. Comparisons between groups were performed by Student's t test. $^{**}p < 0.01$, $^{***}p < 0.001$. (D, E, F) IFN-α2a treatment induces IFITM protein expression and inhibits PRV Bartha-61 infection in PK15 cells. The protein expression of IFITM in PK15 cells pretreated with IFN-α2a (5000 IU/mL, 10,000 IU/mL and 15,000 IU/mL) was detected by western blotting respectively. Cell samples were collected and RIPA lysis for 30min on ice. Then centrifuged for 15 min at 4°C to remove cell debris. Cell extracts were mixed with reducing loading buffer and electrophoresed by SDS-polyacrylamide (SDS-PAGE) on a 15 % polyacrylamide gel. All samples were heated at 95°C for 5 min prior to being loaded onto an SDS-PAGE gel. After electro blotting the separated proteins onto a Polyvinylidene Fluoride (PVDF) membrane, unspecific antibody binding was blocked with phosphate-buffered saline (PBS)/Tween® 20 containing 2.5 % skimmed milk for 1h at room temperature. Then incubated blots in IFITM1, 2 or 3 specific antibodies 1: 2000 diluted at 4°C overnight. Then washed and incubated with horseradish peroxidase (HRP)-conjugated Goat anti Mouse or Rabbit secondary antibody. Blots were washed three times in PBST and developed with ECL reaction substrate. For all experiments, β-actin served as an internal reference. (G) PK15 cells were pretreated with different concentrations of IFN-α2a (5000 IU/mL, 10,000 IU/mL and 15,000 IU/mL) followed by infection with PRV Bartha-61 strain at 100TCID$_{50}$. Cell culture supernatants were collected at different time points (12 h, 24 h, 36 h and 48 h). The TCID$_{50}$ assay was performed to detect infectious viral particles (Reed − Muench method). Data were expressed as mean ± SD from three independent experiments.

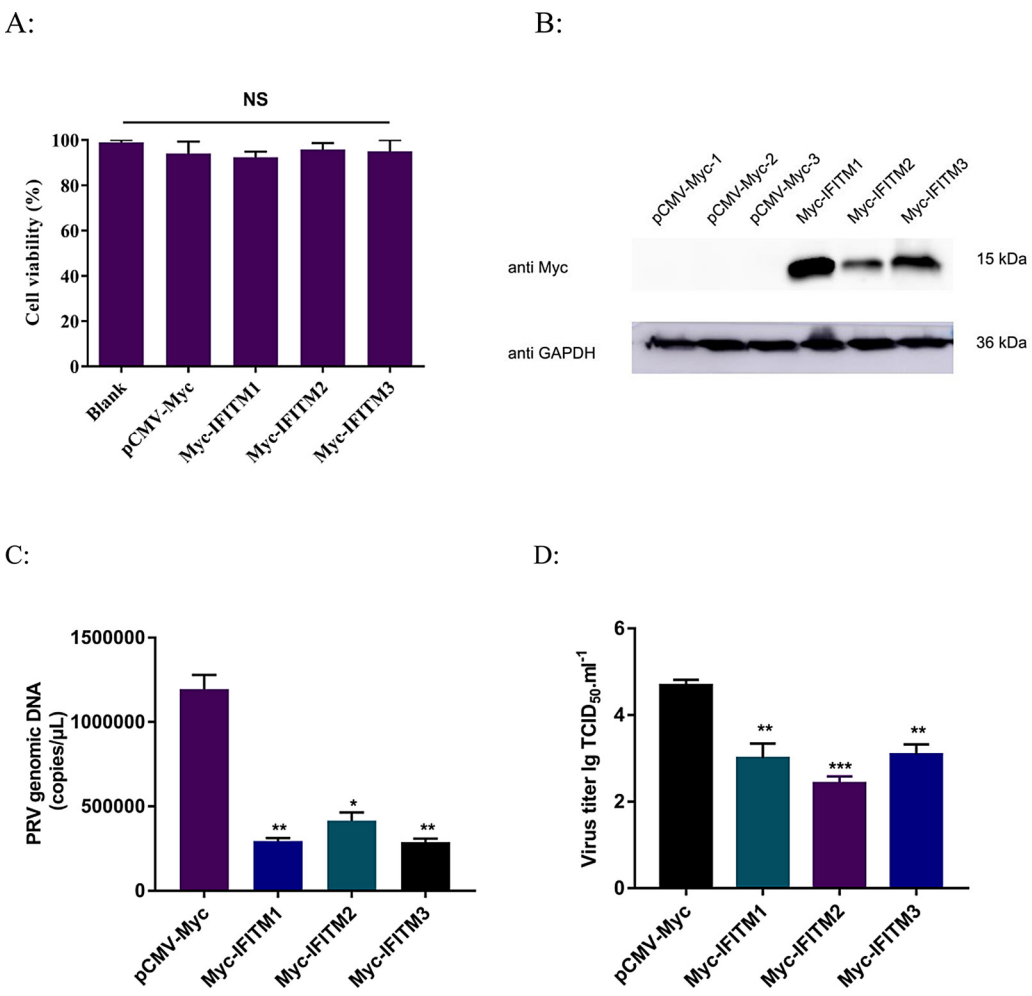

Fig. 2. Overexpression of IFITM proteins suppresses PRV infection in PK15 cells.
(A) PK15/Myc-IFITM cells were cultured in a 96-well plate for 24 h, and the cell viability was determined using the CCK8 reagent. The cell viability of PK15 cells was used as the control. Data were expressed as the mean ± SD from three independent experiments. (B) PK15 cells were transfected with the expression plasmids, Myc-IFITM1, Myc-IFITM2, and Myc-IFITM3 for 24 h, following which the cells were collected for western blotting analysis. An anti-Myc antibody was used and GAPDH served as the loading control. (C) The Myc, Myc-IFITM1, Myc-IFITM2 and Myc-IFITM3 cells were infected with PRV at 100TCID$_{50}$. Culture supernatant was collected at 24 h post infection. And viral DNA was extracted according to manufacture's instruction. PRV genomic DNA copies was detected using real-time TaqMan PCR. (D) Infectious progeny viral titers were determined by the TCID$_{50}$ assay. Data were expressed as mean ± SD from three independent experiments and were measured in technical duplicate. Comparisons between groups were performed by Student's t test. *$p < 0.05$, **$p < 0.01$, ***$p < 0.001$.

and subjected to RT-qPCR using the ABI 7500 Fast Real-Time PCR System (Applied Biosystems). DNA from PRV viral stock was extracted and serial dilutions were used as a quantification control. All experiments were performed using the following amplification profile: one cycle at 94 °C for 30 s and 40 cycles at 94 °C for 5 s and 55.6 °C for 34 s. Primers and probe for PRV real-time TaqMan PCR are listed in Table 1.

2.7. Evaluation of the inhibitory effect of IFITM proteins on PRV infection

PK-15 cells transiently expressing IFITM proteins and control cells were inoculated with PRV at 100TCID$_{50}$ for 2 h, following which the medium was removed and DMEM containing 3 % NBS was added. Cells were harvested 24 hpi. The PRV genomic copies number was detected by RT-qPCR using a pair of primers. For knockdown assays, PK-15 cells were transfected with si-IFITM or si-NC for 24 h using Lipofectamine® 3000 and subsequently inoculated with PRV at 100TCID$_{50}$. The viral titers of the cell supernatants were detected using the TCID$_{50}$ assay in BHK-21 cells.

2.8. Virus binding and entry assay

PRV binding was performed in 6 well plates at 4 °C. PK15 cells overexpressed IFITM proteins were cultures in 6 well plates, virus infection at an multiplicity of infection (MOI of 1) when cell density obtained 80 %. After two hours on ice, cells were washed with ice-cold PBS to remove unbound virus, and samples to measure bound virus were collected by scraping cells into PBS, followed by additional washing. For virus entry study, first binding and washing at 4 °C then incubating samples at 37 °C for two hours in DMEM medium. Cells were then washed with PBS and treated with 0.05 % trypsin and

washed to remove surface bound virus. Samples were kept on ice after the final washing step, then processed for DNA. Primers specific to the PRV genomic DNA detecction were used for RT-qPCR.

2.9. Enzyme-linked immunosorbent assay (ELISA)

PK15 cells were infected with 100TCID$_{50}$ PRV for 12 h and 24 h. IFN-β levels in the cell supernatants were detected using a swine IFN-β ELISA kit (Jianglaibio, Shanghai, China), according to the manufacturer's instructions.

2.10. Evaluation of the cell viability by the CCK-8 assay

According to the manufacturer's instructions, a cell viability assay was performed using the CCK-8 reagent (Beyotime, China). Cells were grown on a 96-well plate and incubated with the enhanced CCK8 reagent for 1 h. The absorbance of the soluble formazan was measured at 450 nm.

2.11. Statistical analysis

Measurements were compared using a one-way ANOVA. Statistical significance comparisons were calculated using a Student's *t*-test. Values are expressed in graph bars as the mean ± SD of at least three independent experiments, unless otherwise noted. Asterisks denote statistically significant differences (*** $p < 0.001$, ** $p < 0.01$ and * $p < 0.05$).

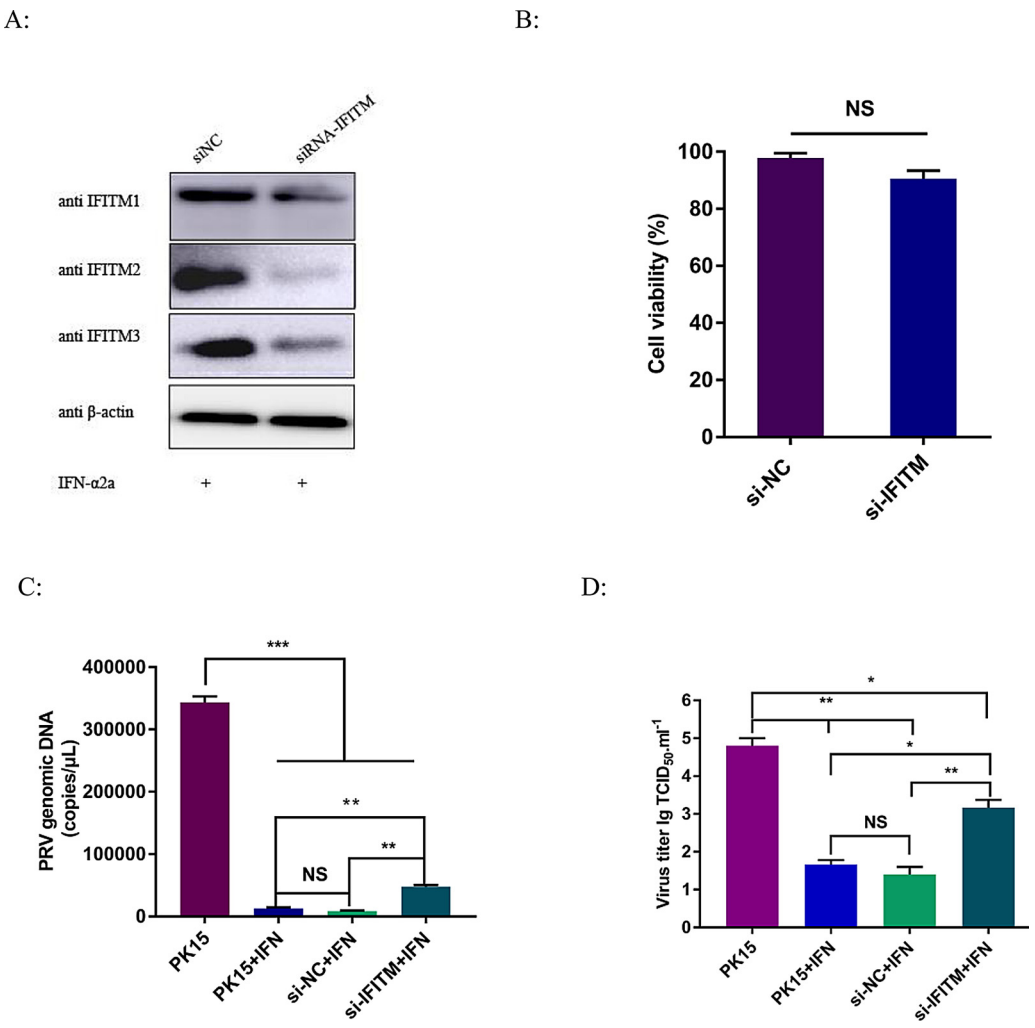

Fig. 3. Knockdown of IFITM protein expression by siRNA promotes PRV replication in PK15 cells.
(A) PK15 cells were pretreated with IFN-α2a 5000 IU/mL for 8 h and subsequently transfected with siRNA targeting IFITMs proteins. After 24 h, IFITM protein expression was analyzed by western blotting using specific antibodies. β-actin served as the loading control. (B) PK15/si-IFITM cells were cultured in a 96-well plate for 24 h, and the cell viability was determined using the CCK8 reagent. Cells treated with a control siRNA (si-NC) was used as the control. Data were expressed as the mean ± SD from three independent experiments. (C) Cells with knocked down IFITMs were infected with PRV at 100$TCID_{50}$ for 24 h, then virus was collected and viral DNA was extracted for PRV genomic DNA copies detection by real-time TaqMan PCR. (D) Infectious progeny viral titers were determined by the $TCID_{50}$ assay. Data were expressed as mean ± SD from three independent experiments and were measured in technical duplicate. Comparisons between groups were performed by Student's t test. $^{*}p < 0.05$, $^{**}p < 0.01$, $^{***}p < 0.001$.

3. Results

3.1. IFITM is crucial for controlling PRV infection

3.1.1. PRV infection and IFN-α2a treatment induces IFITM expression

IFITM proteins are located in different cellular compartments, and their antiviral properties strongly correlate with their capacity to alter the fluidity and fusion ability of the membranes in which they reside (Amini-Bavil-Olyaee et al., 2013; Desai et al., 2014). To see whether PRV can induce IFITM expression, porcine kidney cells, PK15, were infected with PRV at 100$TCID_{50}$ for 12 h and 24 h. Expression of IFITM family members were significantly increased after PRV infection, notably at 24 h post-infection (Fig. 1A). We reason that this could be due to an IFN-mediated event triggered by PRV infection (Fig. 1B and C). Indeed, treatment of PK15 cells with recombinant IFN-α2a induced IFITM1, 2, and 3 protein expression in a dose dependent manner (Fig. 1D, E and F) and dampened PRV infectivity (Fig. 1G).

3.1.2. Overexpression of IFITM proteins suppresses PRV infection in PK15 cells

However, to conclusively show that loss of PRV infectivity was due to increased IFITM protein expression, cells overexpressing IFITM1, 2 and 3 (Fig. 2B) were infected with PRV. PRV DNA copies and viral titer at 24 h post-infection was decreased in IFITM-overexpressed cells (Fig. 2C and D) and was not due to loss of cell viability (Fig. 2A).

3.1.3. Knockdown of IFITM protein expression by siRNA promotes PRV replication in PK15 cells

To evaluate the role of IFITM in IFN antiviral activity against PRV replication, PK15 cells were pretreated with IFN-α2a for 8 h followed by RNAi for 24 h. As swine IFITM1, IFITM2 and IFITM3 has high amino acid similarity (Lanz et al., 2015; Miller et al., 2014), we designed a set of siRNAs targeting IFITM1, IFITM2 and IFITM3. Loss of IFN-induced IFITM family members protein expression by siRNA knockdown (Fig. 3A) significantly increased PRV DNA expression and titers (Fig. 3C and D) without compromising cell viability (Fig. 3B). Overall, we show that IFITM is crucial for PRV replication and infectivity.

Overall, overexpression of IFITM proteins suppresses PRV infection and knockdown IFITM proteins expression by siRNA promotes PRV replication.

3.2. IFITM proteins interfere with PRV binding and entry

To determine the mechanism of anti-PRV activity by IFITM, we examined whether PRV attachment and entry could be obstructed by overexpression of IFITM proteins in PK15 cells. To analyze viral binding, PK15 cells were incubated with PRV at 4 °C for 2 h to achieve viral attachment but restrict viral entry. The excess virus was then washed away and viral DNA was extracted, representing only PRV bound to the cell surface. Only IFITM2 had an effect on PRV cell binding (Fig. 4A). To assess viral entry, PK15 cells were subjected to incubation at 37 °C for an additional 2 h to allow PRV to enter the cells. Indeed, the presence of overexpressed IFITM proteins decreased PRV

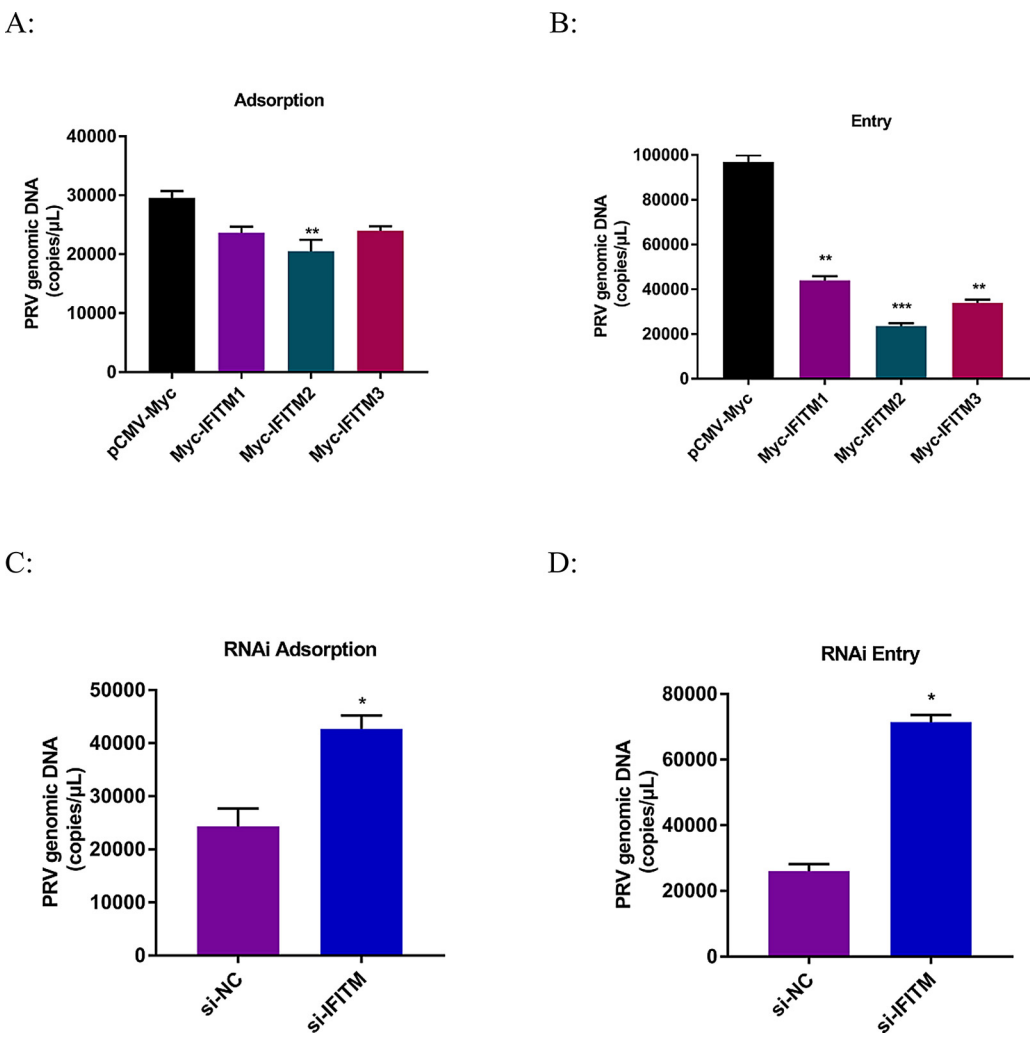

Fig. 4. IFITM proteins restrict PRV entry into PK15 cells.
PK15 cells overexpressing or knockdown of IFITM proteins were applied to viral adsorption and entry experiments. Cells were infected with PRV at an MOI of 1. (A,C) For the adsorption assay, cells were incubated at 4 ˚C for 2 h, washed 4 times with cold PBS and collected for DNA extraction. Real-time PCR was used to detect the virus copies bound to the cell surface. (B,D) For the entry assay, cells were incubated at 37 ˚C for another 2 h, washed 4 times with cold PBS and collected for DNA extraction. The viral entry into cells was detected by real-time TaqMan PCR. Data were expressed as mean ± SD from three independent experiments and were measured in technical duplicate. Comparisons between groups were performed by Student's t test. $*p < 0.05$, $**p < 0.01$.

DNA (Fig. 4B) suggesting that IFITM proteins interfere with PRV cell entry. We also carried out virus adsorption and entry experiments on IFITM proteins knockdown cell lines (Fig. 4C and D), these results further proved that IFITM proteins could inhibit the process of viral attachment and entry.

3.3. IFITM2-mediated inhibition of PRV entry requires cholesterol

Cellular lipid membranes are involved in regulating the entry and release of many viruses. Cholesterol is essential in lipid raft membranes. Numerous studies have demonstrated cholesterol have requisite functions in viral infection (Chang et al., 2012; Gianni and Campadelli-Fiume, 2012; Schroeder, 2010). Modulation of intracellular cholesterol homeostasis within cells, especially in the endosomal compartment, has significant effects on the entry stage of viral infection (Carette et al., 2011; Poh et al., 2012). To examine the impact of cholesterol depletion on viral infectivity we infected cells pre-incubated for 45 min with different concentrations of Methyl-β-cyclodextrin (MβCDX), a cholesterol-removing agent, with 100$TCID_{50}$ PRV for 2 h, then replaced with 3 % NBS DMEM medium. We confirmed that MβCDX was not toxic on PK15 cells (Fig. 5A). Compared with control cells, viral titers in MβCDX treated cells were much lower, indicating that PRV infectivity is dependent on cholesterol (Fig. 5B). Furthermore, the use of cholesterol pathway inhibitor, PF429242 (Hawkins et al., 2008), caused a dose-dependent reduction in PRV titer (Fig. 5D), with no effect on cell viability (Fig. 5C). As IFITM2 interferes with both PRV cell binding and entry (Fig. 4 A and B), we assessed whether this process was dependent on cholesterol. Cells overexpressing IFITM2 were treated with PF429242 for 24 h before infecting with PRV. IFITM2-mediated antiviral effect was weakened in the presence of PF429242 (Fig. 5E and F). We also did viral binding and entry assays to assess the association between cholesterol inhibition and IFITM2 on viral entry. The presence of PF429242 destroyed the inhibition of IFITM2 on virus adsorption and entry (Fig. 5G and H) suggesting that the cholesterol pathway is essential for IFITM-mediated suppression of PRV infectivity.

4. Discussion

Most ISGs, including IFITM, promote innate immunity against viral infection and contribute to the antiviral activity of IFNs (Brass et al., 2009; Xue et al., 2016). Among IFITM family members, IFITM1, 2 and 3 are well studied. IFITM proteins have been shown to broadly suppress viral infection by changing membrane fluidity or physical properties of cell membranes, or by changing properties of the cytoplasm or lumina (Amini-Bavil-Olyaee et al., 2013; Bailey et al., 2013; Li et al., 2013; Nan et al., 2017;). While different IFITM proteins have been repeatedly described in defense against RNA viruses, their role against DNA viruses are poorly understood.

Swine IFITM proteins have been shown to inhibit RNA virus infectivity including, influenza A (Lanz et al., 2015), classical swine fever (Li et al., 2019) and foot-and-mouth disease (Xu et al., 2014) viruses. Though porcine IFITM1 was previously shown to be required for PRV infectivity (Wang et al., 2019), our study extends this observation to other family members including IFITM 2 and 3. We confirm that all

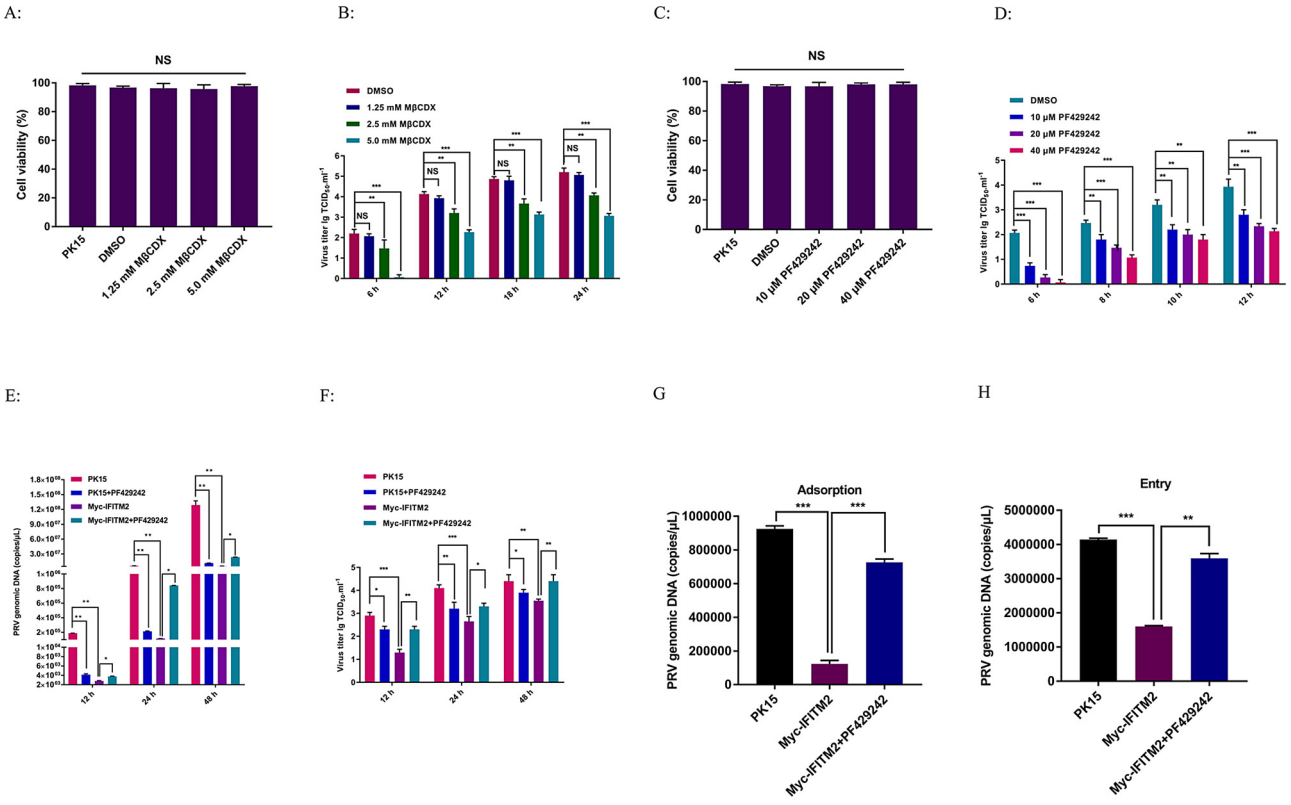

Fig. 5. IFITM2 inhibit PRV entry maybe required the accumulation of cholesterol.
(A,C) Chemicals were previously tested for cytotoxicity at the concentrations used. PK15 cells treated with 1.25 mM, 2.5 mM and 5.0 mM Methyl-β-cyclodextrin (MβCDX) for 45 min in 96 well plate. For cholesterol inhibitor PF429242, cells were pretreated with 10 μM, 20 μM and 40 μM PF429242 for 24 h then following other experimental operations. Cell viability was determined using the CCK8 reagent according to manufacture's instruction. Data were expressed as the mean ± SD from three independent experiments. (B,D) Infection of cells pretreated with (B) MβCDX and (D) PF429242 blocks infection with PRV Bartha-61 strain. PK15 cells were pretreated with DMSO, MβCDX or PF429242 at the indicated concentrations and hours, subsequently cells were infected with virus at 100$TCID_{50}$ for 2 h and then overlaid with fresh media. All infections and incubations were carried out in the presence of indicated concentrations of PF429242, but not conclude MβCDX. For MβCDX treated cells, infection culture supernatant was collected at 6 h, 12 h, 18 h and 24 h. PF429242 treated cells supernatant was collected at 6 h, 8 h, 10 h and 12 h after PRV infection. All sampleswere used for $TCID_{50}$ assay. Values were compared to viral titer of DMSO treated cells. Data were expressed as mean ± SD from three independent experiments. (E) PK15 cells infected with 100$TCID_{50}$ PRV, PK15 cells pretreated with 20 μM PF429242 following 100$TCID_{50}$ PRV infection, IFITM2 overexpressed cells infected with 100$TCID_{50}$ PRV and IFITM2 overexpressed cells pretreated with 20 μM PF429242 following 100$TCID_{50}$ PRV infection were performed and cell culture supernatant was collected at 12 h, 24 h and 48 h for viral DNA extraction. Then Real-time PCR was performed for viral DNA copies detection. PK15 cells infected with PRV alone served as control. Data were expressed as mean ± SD from three independent experiments and were measured in technical duplicate. (F) Viral titers of above virus at 12 h, 24 h and 48 h were detected by $TCID_{50}$ assay. PK15 cells infected with PRV alone served as control. Data were expressed as mean ± SD from three independent experiments. (G, H) IFITM2 overexpressed cells untreated or pretreated with 20 μM PF429242 were applied to viral adsorption and entry experiments. Cells were infected with PRV at an MOI of 3. (G) For the adsorption assay, cells were incubated at 4 °C for 2 h, washed 4 times with cold PBS and collected for DNA extraction. Real-time PCR was used to detect the virus copies bound to the cell surface. (H) For the entry assay, cells were incubated at 37 °C for another 2 h, washed 4 times with cold PBS and collected for DNA extraction. The viral entry into cells was detected by real-time TaqMan PCR. Data were expressed as mean ± SD from three independent experiments and were measured in technical duplicate. Comparisons between groups were performed by Student's t test. $*p < 0.05$, $**p < 0.01$, $***p < 0.001$.

three IFITM proteins can influence PRV cellular entry. However, only IFITM2 had a significant impact on both PRV cell binding and entry. IFITM proteins can act at any stage of viral entry, such as directly binding to the virus, blocking receptor access (Liu et al., 2018) or by inhibiting endocytosis thereby preventing membrane fusion or vesicular trafficing (Chesarino et al., 2014; Hoffmann et al., 2015; Weston et al., 2016). Furthermore, we show that IFITM2-mediated inhibition of PRV entry requires cholesterol by the use of cholesterol removing agents and cholesterol pathway inhibitors. IFITM1 has been found to colocalize with early endolysosome markers (Mudhasani et al., 2013; Weston et al., 2014). IFITM2 and IFITM3 also colocalize with endosomal markers but are found in endosomal and lysosomal compartments different to that of IFITM1 (i.e. Rab7, CD63, lysosomal-associated membrane protein (LAMP1)) (Bailey et al., 2014; Jia et al., 2014; Lu et al., 2011; Mudhasani et al., 2013). It is possible that IFITM proteins may be associated with cholesterol as they share the same subcellular location. Vesicle-membrane-protein-associated protein A (VAPA) and oxysterol-binding protein (OSBP) regulates intracellular cholesterol homeostasis and is known to be required by viruses during infection. Indeed, IFITM3 is known to interact with VAPA thereby disrupting intracellular cholesterol homeostasis and inhibiting infuenza virus A entry (Amini-Bavil-Olyaee et al., 2013). Though our current data may suggest IFITM2 inhibition of PRV proliferation via the cholesterol pathway, whether this occurs via VAPA remains to be seen. IFITM proteins are type I IFN inducible (i.e. ISGs) and ISGs are known to control viral infectivity (Schoggins et al., 2011). Though data shows that PRV infectivity in PK15 cells is significantly affected by IFN treatment, we have yet to conclusively show whether this is due to IFN-induced increased activity of IFITMs. Nonetheless, we show that IFITM overexpression dampens PRV infectivity. Indeed, another ISG family member, ISG15, has been shown to enhance the IFN-β response to inhibit the replication of PRV in PK15 cells (Liu et al., 2018).

In conclusion, we show that IFITM proteins play a vital role in controlling PRV infectivity. The exact mechanism by which IFITM

proteins inhibit PRV infection is still unclear; nevertheless, our results illustrate a relationship between the IFITM proteins and the cholesterol pathway, which is necessary for PRV infection. Thus, IFITM1, 2 and 3 can be considered potential anti-PRV effectors that protect the host from infection. The present study improves our understanding of the antiviral role of IFITMs in PRV infection and broadens its role to anti-DNA viral infection.

CRediT authorship contribution statement

Jingying Xie: Investigation, Methodology, Formal analysis, Writing - original draft. **Yingjie Bi:** Investigation, Methodology, Formal analysis. **Shujuan Xu:** Investigation, Resources. **Yumei Han:** Investigation, Methodology. **Adi Idris:** Resources, Writing - review & editing. **Haixia Zhang:** Investigation, Resources. **Xiangrong Li:** Investigation, Resources, Methodology. **Jialin Bai:** Software, Funding acquisition. **Yong Zhang:** Resources, Funding acquisition. **Ruofei Feng:** Supervision, Project administration, Funding acquisition.

Declaration of Competing Interest

The authors have no conflicts of interest to declare.

Acknowledgements

This work was supported by the Fundamental Research Funds for the Central Universities (Grant no. 31920190003), the Program for Young Talent of SEAC(Grant no. [2018]98), the National Natural Science Foundation of China (Grant no. 31460665), Open Funds of the Biomedical Research Center from Northwest Minzu University (Grant no. EB201801) and the Changjiang Scholars and Innovative Research Team at the University (Grant no. IRT_17R88).

References

Amini-Bavil-Olyaee, S., Choi, Y.J., Lee, J.H., Shi, M., Huang, I.C., Farzan, M., Jung, J.U., 2013. The antiviral effector IFITM3 disrupts intracellular cholesterol homeostasis to block viral entry. Cell Host Microbe 13 (4), 452–464.

Bailey, C.C., Kondur, H.R., Huang, I.C., Farzan, M., 2013. Interferon-induced transmembrane protein 3 is a type II transmembrane protein. J. Biol. Chem. 288 (45), 32184–32193.

Bailey, C.C., Zhong, G., Huang, I.C., Farzan, M., 2014. IFITM-family proteins: the cell's first line of antiviral defense. Annu. Rev. Virol. 1, 261–283.

Bedford, J.G., O'Keeffe, M., Reading, P.C., Wakim, L.M., 2019. Rapid interferon independent expression of IFITM3 following T cell activation protects cells from influenza virus infection. PLoS One 14 (1), e0210132.

Brass, A.L., Huang, I.C., Benita, Y., John, S.P., Krishnan, M.N., Feeley, E.M., Ryan, B.J., Weyer, J.L., van der Weyden, L., Fikrig, E., Adams, D.J., Xavier, R.J., Farzan, M., Elledge, S.J., 2009. The IFITM proteins mediate cellular resistance to influenza A H1N1 virus, West Nile virus, and dengue virus. Cell 139 (7), 1243–1254.

Carette, J.E., Raaben, M., Wong, A.C., Herbert, A.S., Obernosterer, G., Mulherkar, N., Kuehne, A.I., Kranzusch, P.J., Griffin, A.M., Ruthel, G., Dal Cin, P., Dye, J.M., Whelan, S.P., Chandran, K., Brummelkamp, T.R., 2011. Ebola virus entry requires the cholesterol transporter Niemann-Pick C1. Nature 477 (7364), 340–343.

Chang, T.H., Segovia, J., Sabbah, A., Mgbemena, V., Bose, S., 2012. Cholesterol-rich lipid rafts are required for release of infectious human respiratory syncytial virus particles. Virology 422 (2), 205–213.

Chesarino, N.M., McMichael, T.M., Hach, J.C., Yount, J.S., 2014. Phosphorylation of the antiviral protein interferon-inducible transmembrane protein 3 (IFITM3) dually regulates its endocytosis and ubiquitination. J. Biol. Chem. 289 (17), 11986–11992.

Christensen, L.S., Medveczky, I., Strandbygaard, B.S., Pejsak, Z., 1992. Characterization of field isolates of suid herpesvirus 1 (Aujeszky's disease virus) as derivatives of attenuated vaccine strains. Arch. Virol. 124 (3–4), 225–234.

Desai, T.M., Marin, M., Chin, C.R., Savidis, G., Brass, A.L., Melikyan, G.B., 2014. IFITM3 restricts influenza A virus entry by blocking the formation of fusion pores following virus-endosome hemifusion. PLoS Pathog. 10 (4), e1004048.

Diamond, M.S., Farzan, M., 2013. The broad-spectrum antiviral functions of IFIT and IFITM proteins. Nat. Rev. Immunol. 13 (1), 46–57.

Friedman, R.L., Manly, S.P., McMahon, M., Kerr, I.M., Stark, G.R., 1984. Transcriptional and posttranscriptional regulation of interferon-induced gene expression in human cells. Cell 38 (3), 745–755.

Gianni, T., Campadelli-Fiume, G., 2012. αVβ3-integrin relocalizes nectin1 and routes herpes simplex virus to lipid rafts. J. Virol. 86 (5), 2850–2855.

Hawkins, J.L., Robbins, M.D., Warren, L.C., Xia, D., Petras, S.F., Valentine, J.J., Varghese, A.H., Wang, I.K., Subashi, T.A., Shelly, L.D., Hay, B.A., Landschulz, K.T., Geoghegan, K.F., Harwood, H.J.Jr., 2008. Pharmacologic inhibition of site 1 protease activity inhibits sterol regulatory element-binding protein processing and reduces lipogenic enzyme gene expression and lipid synthesis in cultured cells and experimental animals. J. Pharmacol. Exp. Ther. 326 (3), 801–808.

Hoffmann, H.H., Schneider, W.M., Rice, C.M., 2015. Interferons and viruses: an evolutionary arms race of molecular interactions. Trends Immunol. 36 (3), 124–138.

Huang, I.C., Bailey, C.C., Weyer, J.L., Radoshitzky, S.R., Becker, M.M., Chiang, J.J., Brass, A.L., Ahmed, A.A., Chi, X., Dong, L., Longobardi, L.E., Boltz, D., Kuhn, J.H., Elledge, S.J., Bavari, S., Denison, M.R., Choe, H., Farzan, M., 2011. Distinct patterns of IFITM-mediated restriction of filoviruses, SARS coronavirus, and influenza A virus. PLoS Pathog. 7 (1), e1001258.

Jia, R., Xu, F., Qian, J., Yao, Y., Miao, C., Zheng, Y.M., Liu, S.L., Guo, F., Geng, Y., Qiao, W., Liang, C., 2014. Identification of an endocytic signal essential for the antiviral action of IFITM3. Cell. Microbiol. 16 (7), 1080–1093.

Jiang, D., Weidner, J.M., Qing, M., Pan, X.B., Guo, H., Xu, C., Zhang, X., Birk, A., Chang, J., Shi, P.Y., Block, T.M., Guo, J.T., 2010. Identification of five interferon-induced cellular proteins that inhibit west nile virus and dengue virus infections. J. Virol. 84 (16), 8332–8341.

Lamote, J.A.S., Kestens, M., Van Waesberghe, C., Delva, J., De Pelsmaeker, S., Devriendt, B., Favoreel, H.W., 2017. The pseudorabies virus glycoprotein gE/gI complex suppresses type I interferon production by plasmacytoid dendritic cells. J. Virol. 91 (7), e02276–16.

Lanz, C., Yángüez, E., Andenmatten, D., Stertz, S., 2015. Swine interferon-inducible transmembrane proteins potently inhibit influenza A virus replication. J. Virol. 89 (1), 863–869.

Lewin, A.R., Reid, L.E., McMahon, M., Stark, G.R., Kerr, I.M., 1991. Molecular analysis of a human interferon-inducible gene family. Eur. J. Biochem. 199 (2), 417–423.

Li, K., Markosyan, R.M., Zheng, Y.M., Golfetto, O., Bungart, B., Li, M., Ding, S., He, Y., Liang, C., Lee, J.C., Gratton, E., Cohen, F.S., Liu, S.L., 2013. IFITM proteins restrict viral membrane hemifusion. PLoS Pathog. 9 (1), e1003124.

Li, C., Zheng, H., Wang, Y., Dong, W., Liu, Y., Zhang, L., Zhang, Y., 2019. Antiviral role of IFITM proteins in classical swine fever virus infection. Viruses 11 (2) pii: E126.

Liao, Y., Goraya, M.U., Yuan, X., Zhang, B., Chiu, S.H., Chen, J.L., 2019. Functional involvement of interferon-inducible transmembrane proteins in antiviral immunity. Front. Microbiol. 10, 1097.

Liu, H., Li, S., Yang, X., Wang, X., Li, Y., Wang, C., Chen, L., Chang, H., 2018. Porcine ISG15 modulates the antiviral response during pseudorabies virus replication. Gene 679, 212–218.

Lu, J., Pan, Q., Rong, L., He, W., Liu, S.L., Liang, C., 2011. The IFITM proteins inhibit HIV-1 infection. J. Virol. 85 (5), 2126–2137.

Marcaccini, A., López Peña, M., Quiroga, M.I., Bermúdez, R., Nieto, J.M., Alemañ, N., 2008. Pseudorabies virus infection in mink: a host-specific pathogenesis. Vet. Immunol. Immunopathol. 124 (3–4), 264–273.

Miller, L.C., Jiang, Z., Sang, Y., Harhay, G.P., Lager, K.M., 2014. Evolutionary characterization of pig interferon-inducible transmembrane gene family and member expression dynamics in tracheobronchial lymph nodes of pigs infected with swine respiratory disease viruses. Vet. Immunol. Immunopathol. 159 (3–4), 180–191.

Miller, J.L., Weed, D.J., Lee, B.H., Pritchard, S.M., Nicola, A.V., 2019. Low-pH endocytic entry of the porcine alphaherpesvirus pseudorabies virus. J. Virol. 93 (2) pii: e01849-18.

Mudhasani, R., Tran, J.P., Retterer, C., Radoshitzky, S.R., Kota, K.P., Altamura, L.A., Smith, J.M., Packard, B.Z., Kuhn, J.H., Costantino, J., Garrison, A.R., Schmaljohn, C.S., Huang, I.C., Farzan, M., Bavari, S., 2013. IFITM-2 and IFITM-3 but not IFITM-1 restrict Rift Valley fever virus. J. Virol. 87 (15), 8451–8464.

Müller, T., Hahn, E.C., Tottewitz, F., Kramer, M., Klupp, B.G., Mettenleiter, T.C., Freuling, C., 2011. Pseudorabies virus in wild swine: a global perspective. Arch. Virol. 156 (10), 1691–1705.

Muñoz-Moreno, R., Cuesta-Geijo, M.Á., Martínez-Romero, C., Barrado-Gil, L., Galindo, I., García-Sastre, A., Alonso, C., 2016. Antiviral role of IFITM proteins in african swine fever virus infection. PLoS One 11 (4), e0154366.

Nan, Y., Wu, C., Zhang, Y.J., 2017. Interplay between Janus Kinase/Signal transducer and activator of transcription signaling activated by type I interferons and viral antagonism. Front. Immunol. 8, 1758.

Perreira, J.M., Chin, C.R., Feeley, E.M., Brass, A.L., 2013. IFITMs restrict the replication of multiple pathogenicviruses. J. Mol. Biol. 425 (24), 4937–4955.

Petersen, J., Drake, M.J., Bruce, E.A., Riblett, A.M., Didigu, C.A., Wilen, C.B., Malani, N., Male, F., Lee, F.H., Bushman, F.D., Cherry, S., Doms, R.W., Bates, P., Briley, K.Jr., 2014. The major cellular sterol regulatory pathway is required for Andes virus infection. PLoS Pathog. 10 (2), e1003911.

Poh, M.K., Shui, G., Xie, X., Shi, P.Y., Wenk, M.R., Gu, F., 2012. U18666A, an intracellular cholesterol transport inhibitor, inhibits dengue virus entry and replication. Antiviral Res. 93 (1), 191–198.

Pomeranz, L.E., Reynolds, A.E., Hengartner, C.J., 2005. Molecular biology of pseudorabies virus: impact on neurovirology and veterinary medicine. Microbiol. Mol. Biol. Rev. 69 (3), 462–500.

Reid, L.E., Brasnett, A.H., Gilbert, C.S., Porter, A.C., Gewert, D.R., Stark, G.R., Kerr, I.M., 1989. A single DNA response element can confer inducibility by both alpha- and gamma-interferons. Proc Natl Acad Sci U S A 86 (3), 840–844.

Savidis, G., Perreira, J.M., Portmann, J.M., Meraner, P., Guo, Z., Green, S., Brass, A.L., 2016. The IFITMs inhibit zika virus replication. Cell Rep. 15 (11), 2323–2330.

Schoggins, J.W., Wilson, S.J., Panis, M., Murphy, M.Y., Jones, C.T., Bieniasz, P., Rice, C.M., 2011. A diverse range of gene products are effectors of the type I interferon antiviral response. Nature 472 (7344), 481–485.

Schroeder, C., 2010. Cholesterol-binding viral proteins in virus entry and morphogenesis. Subcell. Biochem. 51, 77–108.

Szpara, M.L., Tafuri, Y.R., Parsons, L., Shamim, S.R., Verstrepen, K.J., Legendre, M.,

Enquist, L.W., 2011. A wide extent of inter-strain diversity in virulent and vaccine strains of alphaherpesviruses. PLoS Pathog. 7 (10), e1002282.
Vannier, P., 1985. Experimental infection of fattening pigs with pseudorabies (Aujeszky's disease) virus: efficacy of attenuated live- and inactivated-virus vaccines in pigs with or without passive immunity. Am. J. Vet. Res. 46 (7), 1498–1502.
Wang, X., Li, C., Zhou, L., Zhang, N., Wang, X., Ge, X., Guo, X., Yang, H., 2014. Porcine reproductive and respiratory syndrome virus counteracts the porcine intrinsic virus restriction factors-IFITM1 and Tetherin in MARC-145 cells. Virus Res. 191, 92–100.
Wang, J., Wang, C.F., Ming, S.L., Li, G.L., Zeng, L., Wang, M.D., Su, B.Q., Wang, Q., Yang, G.Y., Chu, B.B., 2019. Porcine IFITM1 is a host restriction factor that inhibits pseudorabies virus infection. Int J Biol Macromol pii S0141-8130(19)36423-2.
Warren, C.J., Griffin, L.M., Little, A.S., Huang, I.C., Farzan, M., Pyeon, D., 2014. The antiviral restriction factors IFITM1, 2 and 3 do not inhibit infection of human papillomavirus, cytomegalovirus and adenovirus. PLoS One 9 (5), e96579.
Weston, S., Czieso, S., White, I.J., Smith, S.E., Kellam, P., Marsh, M., 2014. A membrane topology model for human interferon inducible transmembrane protein 1. PLoS One 9 (8), e104341.
Weston, S., Czieso, S., White, I.J., Smith, S.E., Wash, R.S., Diaz-Soria, C., Kellam, P., Marsh, M., 2016. Alphavirus restriction by IFITM proteins. Traffic 17 (9), 997–1013.
Wilkins, C., Woodward, J., Lau, D.T., Barnes, A., Joyce, M., McFarlane, N., McKeating, J.A., Tyrrell, D.L., Gale, M.Jr., 2013. IFITM1 is a tight junction protein that inhibits hepatitis C virus entry. Hepatology 57 (2), 461–469.
Xu, J., Qian, P., Wu, Q., Liu, S., Fan, W., Zhang, K., Wang, R., Zhang, H., Chen, H., Li, X., 2014. Swine interferon-induced transmembrane protein, sIFITM3, inhibits foot-and-mouth disease virus infection in vitro and in vivo. Antiviral Res. 109, 22–29.
Xue, B., Yang, D., Wang, J., Xu, Y., Wang, X., Qin, Y., Tian, R., Chen, S., Xie, Q., Liu, N., Zhu, H., 2016. ISG12a restricts hepatitis C virus infection through the ubiquitination-dependent degradation pathway. J. Virol. 90 (15), 6832–6845.
Yang, S., Pei, Y., Zhao, A., 2017. iTRAQ-based proteomic analysis of porcine kidney epithelial PK15 cells infected with pseudorabies virus. Sci. Rep. 7, 45922.
Yu, X., Zhou, Z., Hu, D., Zhang, Q., Han, T., Li, X., Gu, X., Yuan, L., Zhang, S., Wang, B., Qu, P., Liu, J., Zhai, X., Tian, K., 2014. Pathogenic pseudorabies virus, China, 2012. Emerg Infect Dis 20 (1), 102–104.
Zhao, X., Li, J., Winkler, C.A., An, P., Guo, J.T., 2018. IFITM genes, variants, and their roles in the control and pathogenesis of viral infections. Front. Microbiol. 9, 3228.
Zhu, R., Wang, J., Lei, X.Y., Gui, J.F., Zhang, Q.Y., 2013. Evidence for Paralichthys olivaceus IFITM1 antiviral effect by impeding viral entry into target cells. Fish Shellfish Immunol. 35 (3), 918–926.